Journal of the Ceramic Society of Japan 118 [12] 1135-1139 2010 Paper

Tailoring microwave dielectric properties of $BaTi_4O_9$ ceramics by addition of Sm_2O_3

Xianli HUANG,[*,] Ying SONG,[**] Fuping WANG[*,**,†] and E ZHANG[***]**

[*]Department of Applied Chemistry, Nanjing University of Aeronautics and Astronautics, Nanjing 210016, China
[**]Department of Applied Chemistry, Harbin Institute of Technology, Harbin 150001, China
[***]Department of Mathematics, Harbin Vocational College of Science and Technology, Harbin 150301, China

$BaTi_4O_9$ ceramics with Sm_2O_3 addition were prepared in a form of xSm_2O_3+$BaTi_4O_9$ ($x = 1, 3, 5, 7$ mol %) and the microstructures and microwave dielectric properties of the ceramic samples were characterized. SEM shows when x greater than 3 mol %, $BaSm_2Ti_4O_{12}$ crystallized in a fiber shape along the crystalline boundary. With the increase of Sm_2O_3 addition, the dielectric constant increases from 36.65 to 39.8, while the quality factor decreases from 28000 to 19000, τ_f from +20.2 to +10.1 ppm/°C. Results of curve fitting of FIRS show extrinsic dielectric loss could account for the increase of dielectric loss, which should be attributed to the substantial increase of Ti^{3+} and Ti^{2+}.

Key-words : Dielectric ceramics, Dielectric loss, Lattice vibration, Titanate

[Received April 30, 2010; Accepted June 17, 2010]

1. Introduction

In the last two decades of 20th century, modern communications have been much speeded up by the rise of microwave dielectric resonators (MDRs) constructed by microwave dielectric ceramics (MDCs). So far as the MDCs is concerned, after 30 years' development, a serial of pure compounds and composite ceramics with large constants (ε_r), low dielectric loss ($\mathrm{tg}\,\delta$, $Q = 1/\mathrm{tg}\,\delta$, Q: quality factor) have been adopted, for instance, $BaTi_4O_9$, $Ba_2Ti_9O_{20}$, $Sn_{0.2}(Ti_{1-x}Zr_x)_{0.8}O_2$ and $Ba(M'_{1/3}M''_{2/3})O_3$ ($M' = Zn$ and Mg; $M'' = Nb$ and Ta).[1)–4)]

Accompanying the development of the dielectric ceramics is the rapid progress of communications technology, which demands much more high-performance dielectric ceramic systems. Composite ceramics technique provides a promising tool to design dielectric ceramics composites with adjustable dielectric properties. Some dielectric solid solution or composite ceramics such as $CaTiO_3$-based ceramics were developed for microwave applications.[5)–8)]

$BaTi_4O_9$ and $BaSm_2Ti_4O_{12}$ have long been investigated as single-phased ceramics because of their excellent dielectric properties. $BaTi_4O_9$ ceramics possesses a moderate ε_r (~38), low dielectric loss ($Qf > 20000$, where Q is quality factor; $Q = 1/\mathrm{tg}\,\delta$), and a positive τ_f.[2)] In the lanthanide solid solution, only the Sm-containing compounds possess a negative τ_f, together with low dielectric loss ($Qf > 5000$) and a large ε_r (~80).[9)]

Generally, the dielectric properties of mixed-phased composites could be written as:

$$\ln \varepsilon = \sum v_i \ln \varepsilon_i \quad (1)$$

$$\tan \delta = \sum v_i \tan \delta_i \quad (2)$$

$$\tau_f = \sum v_i \tau_{fi} \quad (3)$$

where v_i is the molar ratio of the ith phase; ε_i, $\tan \delta_i$ and τ_{fi} are the dielectric constant, the dielectric loss and the temperature coefficient of the ith phase, respectively. The Formulas indicts that the composite could combine the excellent dielectric properties of at least 2 compounds, so the composite method is successful in elongating the list of dielectric ceramics.

Therefore, in this article, we attempted to prepare a composite dielectric ceramics, in which small amount of Sm_2O_3 addition (1–7 mol %) was used to adjust the dielectric properties of $BaTi_4O_9$. Many authors paid their attentions to modifying the microwave dielectric properties of $BaTi_4O_9$ ceramics by doping technique.[10)–12)] Mn^{4+}, Sn^{4+}, Zr^{4+}, Ca^{2+}, Sr^{2+} and Pb^{2+} were doped into the lattice of $BaTi_4O_9$. In a view of atomic configure, these doping elements could be classified into four types: Mn^{4+} with d-electrons, Sn^{4+} and Zr^{4+} with a d^0 or p^0 configure, Ca^{2+} and Sr^{2+} with an s^0 configure and Pb^{2+} with an s^2 configure in their outmost layer of their atoms. Interestingly, the former two could decrease the dielectric loss, but the latter two could increase the dielectric constant and loss, simultaneously. On the other hand, those dopants are all equivalent valence doping elements or acceptor doping elements (e.g., Mn^{4+}, existing as Mn^{3+} or Mn^{2+} in the lattice after a high-temperature heat-treatment) doped into Ba-sites or Ti-sites. Few works were reported concerning an effect of donor doping on the dielectric properties of $BaTi_4O_9$. The microstructure of composite ceramics was characterized by XRD and SEM. The extrinsic or intrinsic dielectric loss was evaluated by the far infrared spectra.

2. Experimental

The raw regents for the sol–gel method are all of A.R grade and used as purchased. A typical process was as followed:[13)] 10 ml tetrabutyl titanate was added slowly to a mixed solution of 50 ml methyloxyl-ethanol and 1 ml acetic acid. The content of Sm_2O_3 was 1, 3, 5 and 7 mol % of that of $BaTi_4O_9$. Stoichiometric $Ba(Ac)_2$ and $Sm(Ac)_3$ was dissolved in a certain amount of water. Under vigorous stirring, the concentrated hydraulic solution was added dropwise to the mixed solution of tetrabutyl titanate, and then the mixed solution turned into a transparent sol. After drying at 60°C for 48 hours, the solution became a dry gel.

† Corresponding author: F. Wang; E-mail: xianlihuang@163.com

The so-obtained gel was calcined at 1200°C for 4 hours to obtain the precursor powder.

The precursor powder was ball-milled for 24 hours and pressed by a 150 MPa cool iso-static press into a disk with a diameter of 12 mm and a thickness of 6 mm. The pressed green bodies were dried in an oven at 80°C for 24 hours, then sintered at 1250–1350°C for 4 or 6 hours.

The densities measurements of the samples were carried out using an Archimedes method. The crystal structure of sintered samples was examined by X-ray powder diffraction with monochromatic Cu Kα_1 radiation (MO 3X HF Mac Science, Tokyo, Japan), as shown in Fig. 2. The ceramic bulks were observed by SEM (Hitachi S4700, Japan) electroscope, and their surfaces were analyzed by XPS (EscalabmkII, VG. Co., U.K.). Before measuring dielectric properties, the ceramics was well polished. The microwave dielectric properties were experimentally determined at 7.5 GHz by the resonant cavity method in the TE_{011} dielectric resonator mode using a HP8363A network analyzer (Agilent, U.S.A.).

IR reflectance spectra were recorded using a Fourier-transform spectrometer (Bruker IFs66v/s) equipped with a fixed-angle specular reflectance accessory (external incidence angle of 11.5°). In the mid-infrared region (400–3000 cm^{-1}), a SiC glow-bar lamp was used as an infrared source along with a Ge-coated KBr beamsplitter and an LN_2-cooled HgCdTe detector. In the far-infrared range (50–500 cm^{-1}), a mercury-arc lamp, a 6 µm coated Mylar hypersplitter, and an LHe-cooled Si bolometer were used. An Au reflector was used as measurement reference, and the spectral resolution was 2.0 cm^{-1}.

The relation between the reflection spectrum and the complex dielectric constant can be written as:

$$R = \left(\left|\frac{\sqrt{\varepsilon}-1}{\sqrt{\varepsilon}+1}\right|\right)^2, \tag{4}$$

where R is the reflectance and ε is the dielectric constant. The latter can be transformed into a dielectric dispersion spectrum using a classical damped dispersion oscillator model:

$$\varepsilon = \varepsilon_\infty \prod_j^n \frac{\Omega_{j\mathrm{Lo}}^2 - \omega^2 + i\omega\gamma_{j\mathrm{Lo}}}{\Omega_{j\mathrm{To}}^2 - \omega^2 + i\omega\gamma_{j\mathrm{To}}}, \tag{5}$$

where ω is the angular frequency; ε is the dielectric constant; $\Omega_{j\mathrm{To}}$, $\Omega_{j\mathrm{Lo}}$, and $\gamma_{j\mathrm{To}}$ $\gamma_{j\mathrm{Lo}}$ are the transverse vibration mode, the longitude vibration mode and the damping coefficients of the jth vibration mode, respectively; and ε_∞ is the high frequency dielectric constant, which was evaluated at 3000 cm^{-1}.

The oscillator strength $\Delta\varepsilon_j$ and the dielectric loss $\mathrm{tg}\,\delta_j$ can then be obtained from

$$\Delta\varepsilon_j = \varepsilon_\infty\left(\frac{\Omega_{j\mathrm{Lo}}^2}{\Omega_{j\mathrm{To}}^2} - 1\right)\prod_{k\neq j}\frac{\Omega_{k\mathrm{Lo}}^2 - \Omega_{j\mathrm{To}}^2}{\Omega_{k\mathrm{To}}^2 - \Omega_{j\mathrm{To}}^2} \tag{6}$$

$$\mathrm{tg}\,\delta_j = \frac{\Delta\varepsilon_j(\gamma_{j\mathrm{To}}\times\omega)}{\Omega_{j\mathrm{To}}^2 \times \left(\varepsilon_\infty + \sum_k \Delta\varepsilon_k\right)} \tag{7}$$

The dielectric constant and loss were calculated using Eqs. (8) and (9):

$$\varepsilon' = \varepsilon_\infty + \sum_j^n \Delta\varepsilon_j \tag{8}$$

$$\mathrm{tg}\,\delta = \sum_j^n \mathrm{tg}\,\delta_j \tag{9}$$

where n is equal to 32 in this study.[14)]

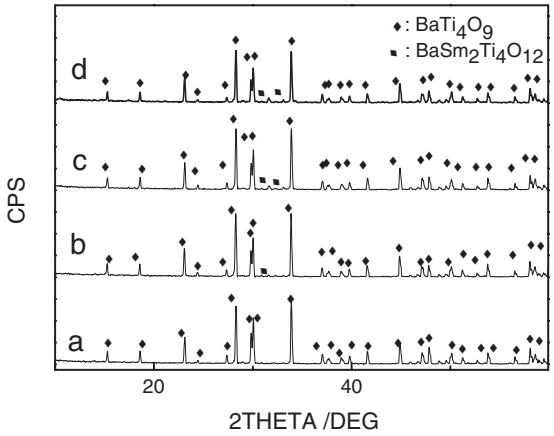

Fig. 1. XRD patterns of 1 mol % (a), 3 mol % (b), 5 mol % (c), 7 mol % (d) Sm-doped $BaTi_4O_9$ ceramics.

3. Results and discussion

3.1 XRD patterns

XRD patterns of ceramic samples were shown in **Fig. 1**. For both patterns of $x = 1$ mol % and $x = 3$ mol %, there existed only $BaTi_4O_9$ phases with a JCPDF No. 34-0070. For the other x larger than 3 mol %, there existed two phases. Besides the main phase of $BaTi_4O_9$, the other phase should be attributed to the pattern of $BaSm_2Ti_4O_{12}$ with a JCPDF No. 44-0062. In the quasi-ternary phase diagram of BaO–TiO_2–Sm_2O_3, $BaTi_4O_9$ and $BaSm_2Ti_4O_{12}$ are two of the most stable compounds.[15)]

Compared with XRD peaks of pure $BaTi_4O_9$, many XRD peaks of Sm_2O_3-doped ceramics shifted toward smaller 2theta, indicating the d values decreased. But, there were no difference for XRD peaks for 1, 3, 5 and 7 mol % samples. This fact might reveal that the solubility of Sm_2O_3 should be lower than 1 mol %.

3.2 Density measurement

The densities of ceramic samples were estimated by a linear weighed addition of two separate phases:

$$d_{\mathrm{theo}} = d_{\mathrm{BT4}} \times (1-x) + d_{\mathrm{BST4}}x \tag{10}$$

d_{theo}: theoretical density calculated by Formula (1); d_{BT4}: theoretical density of $BaTi_4O_9$, 4.54 g/cm^3; d_{BST4}: theoretical density of $BaSm_2Ti_4O_{12}$, 5.80 g/cm^3; x: molar ratio of Sm_2O_3.

The measured and calculated results were shown in **Fig. 2**. All the measured relative densities were larger than 95%. According to Formula (10), the measured densities should increase with x. But in Fig. 2, the measured densities of 1 and 3 mol % Sm_2O_3 doped samples, which should be ascribed to the formation of defects (point defects or grain boundary). When x was larger than 3 mol %, the differences between the measured and calculated densities become larger and larger with increasing of x, indicating crystalline boundary volume between $BaTi_4O_9$ and $BaSm_2Ti_4O_{12}$ increased.

3.3 SEM

The SEM photographs were shown in **Fig. 3**. EDS of 7 mol % Sm_2O_3 doped $BaTi_4O_9$ was carried out to identify the different phases in Fig. 3(D). According to the EDS analysis, the needle-shaped grains (marked by black arrows in Fig. 3(C) had a composition of Ba, Sm and Ti, indicating that those granular should be $BaSm_2Ti_4O_{12}$. The presence of secondary phase might be due to much smaller ionic radii of Sm^{3+} (0.096 nm) and larger

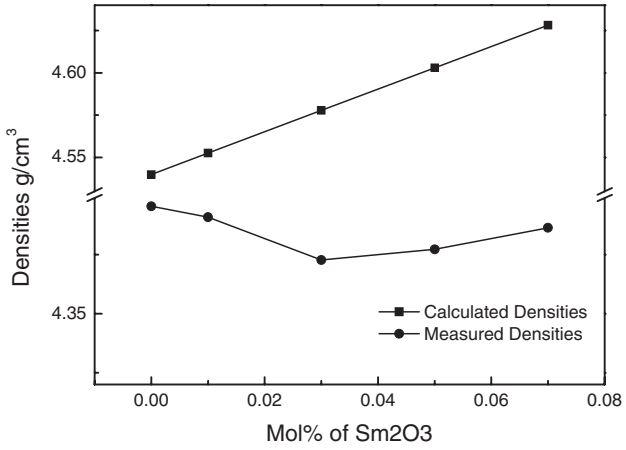

Fig. 2. Measured and relative densities of Sm doped $BaTi_4O_9$ ceramics as a function of concentration of Sm doping.

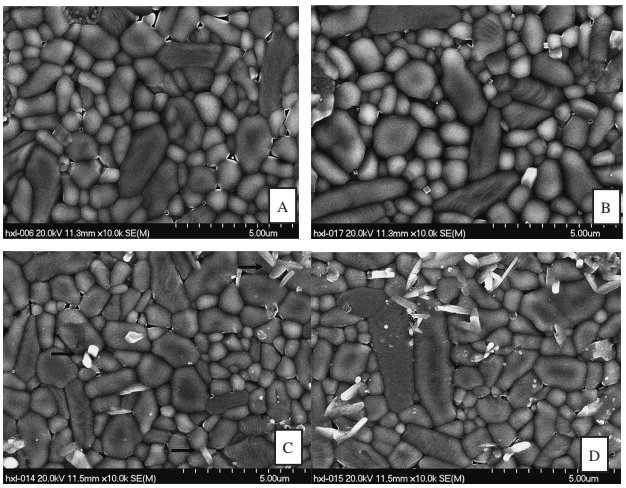

Fig. 3. SEM of 1 mol % (A), 3 mol % (B), 5 mol % (C), 7 mol % (D) Sm-doped $BaTi_4O_9$ ceramics.

ionic charge of Sm^{3+}, compared with that of Ba^{2+} (0.127 nm).[16] $BaSm_2Ti_4O_{12}$ phase first crystallized at the boundary of $BaTi_4O_9$ phases. For those samples with x smaller than 5 mol %, $BaSm_2Ti_4O_{12}$ phase formed in a form of small particles, while for those with $x = 3$ mol %, it existed in a form of needle-like grains.

3.4 Dielectric properties

The dielectric constant, quality factor and temperature coefficients of Sm-doped $BaTi_4O_9$ were shown in **Fig. 4**(a), (b) and (c), respectively. In Fig. 4(a), the dielectric constant increased steadily form 36.65 for undoped sample to 39.8 for $x = 7$ mol %. The variation of dielectric constants could be fitted by the weighed dielectric constant of mixed-phased composite dielectrics. This fact could elucidate that the increase of dielectric constant should be attributed to the presence of $BaSm_2Ti_4O_{12}$.

Figure 4(b) plotted the measured quality factor varied with the molar ratio of Sm_2O_3. For $x = 1$ mol % samples, an abrupt decrease of quality factor was about 25% of Qf values for undoped samples. Such an abrupt increase could not be fitted by the linear weighed dielectric loss of mixed phase dielectrics, which would be discussed in the following paragraphs together with XPS results.

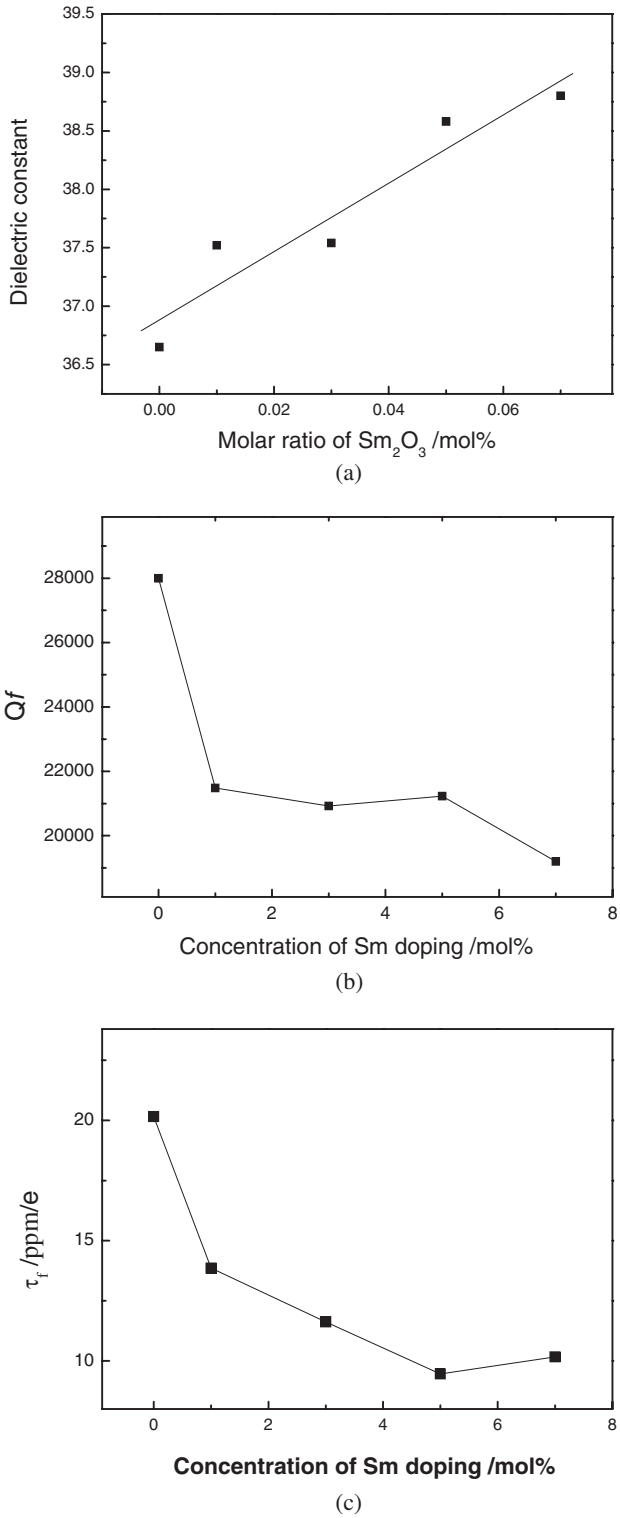

Fig. 4. Variation of dielectric constant (a), dielectric loss (b) and temperature coefficients (c) as a function of the concentration of Sm doping.

The addition of Sm_2O_3 also leaded to a decrease of the temperature coefficient, as shown in Fig. 4(c), because of the negative τ_f of $BaSm_2Ti_4O_{12}$. τ_f reaches to the smallest value of +10.1 ppm/°C at $x = 5$ mol %. However, an abrupt decrease of τ_f about 30% could also be observed for $x = 1$ mol % sample, which might be brought about by variation in microstructure after Sm_2O_3 doping.

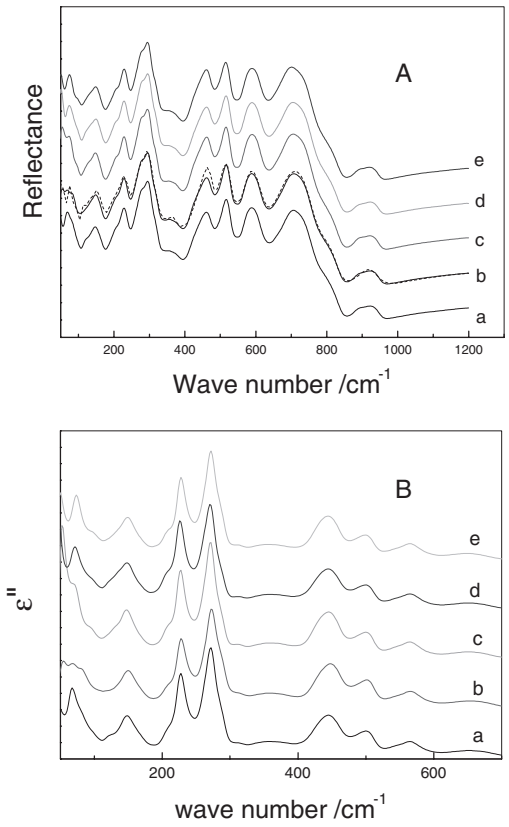

Fig. 5. Far infrared reflectance spectra (A) and ε'' (B) of undoped (a), 1 mol % (b), 3 mol % (c), 5 mol % (d), 7 mol % (d) Sm_2O_3-doped $BaTi_4O_9$ ceramics. (In Fig. 5(a), the dotted line: curve fitting of 1 mol % Sm_2O_3-doped ceramics)

3.5 Far infrared spectra of Sm-doped $BaTi_4O_9$

The dielectric loss could be classified into two types, i.e., eigen dielectric loss and non-eigen dielectric loss. The eigen dielectric loss is induced by non-harmonic effects of lattice vibration, the non-eigen dielectric loss by defects, pores, secondary phases and so on.[13] Far infrared reflectance spectrum (FIRS) is often used to characterize the lattice vibration of microwave dielectric ceramics.[17),18] The FIRS and ε'' of Sm-doped $BaTi_4O_9$ ceramics were shown in **Figs. 5**(A) and (B), respectively.

Figures 5(A) and (B) showed that the vibration modes larger than 100 cm^{-1} kept almost unchanged when doping concentrations vary. But those modes below 100 cm^{-1} concerning Ba–O stretching or scissoring vibration modes vary in a disorderly manner with the increasing of Sm_2O_3 doping. This fact also could attest that some Sm^{3+} ions occupied Ba-sites.

The parameters used in curve-fitting were listed in **Table 1**, and **Table 2**. The calculated dielectric constants and the dielectric loss of 1 mol % Sm-doped $BaTi_4O_9$ ceramics are 38.52 and 1.70E−4, respectively, which agreed very well with those (38.16 and 1.77E−4) of undoped $BaTi_4O_9$ ceramics.[14] This fact indicted that the increase of dielectric loss should not be attributed to the anharmonic effect of vibration modes after Sm_2O_3 doping, but to the microstructural variation introduced by substitution of Ba^{2+} by Sm^{3+}.

3.6 XPS analysis

In order to analyze the microstructural variation of $BaTi_4O_9$ after addition of Sm_2O_3, XPS analysis of undoped or 1% Sm_2O_3 doped samples was carried out, as shown in **Figs. 6**(a) and (b).

Table 1. Parameters used in curve fitting process

jth	Ω_{jTo}	γ_{jTo}	Ω_{jLo}	γ_{jL}	$\mathrm{tg}\,\delta_j \times 10^{-6}$*	$\Delta\varepsilon_j$
1	53.24	8.31	54.31	8.99	20.16	2.05
2	60.05	9.04	61.07	9.06	13.05	1.48
3	67.85	8.71	69.08	8.38	15.82	1.59
4	76.32	8.92	78.09	8.27	11.35	2.12
5	82.59	5.56	84.87	6.37	7.49	1.75
6	90.43	8.82	92.85	8.3	7.70	1.36
7	100.38	15.35	102.53	12.94	8.19	1.02
8	120.76	20.16	123.17	13.17	12.07	1.66
9	129.09	10.74	131.91	10.6	4.70	1.39
10	135.25	8.92	136.85	8.95	1.30	0.51
11	141.04	6.57	142.95	9.05	1.91	1.1011
12	150.2	8.14	153.65	10.47	2.10	1.11
13	158.27	6.83	161.4	8.76	0.82	0.57
14	170.64	19.88	173.69	21.73	2.09	0.58
15	203.99	62.79	205.38	57.82	6.35	0.80
16	209.52	39.64	214.77	50.06	6.42	1.35
17	228.36	15.06	233.36	29.36	1.59	1.05
18	245.3	55.04	252.29	44.41	5.35	1.11
19	267.42	21.79	273.55	80.34	1.56	0.97
20	290.45	27.73	308.68	22.82	3.37	1.95
21	313.82	17.12	316.4	24.72	0.12	0.135
22	321.65	62.65	332.18	55.94	1.03	0.32
23	376.16	63.97	385.56	16.83	2.65	1.11
24	387.84	16.66	395.19	38.9	0.10	0.18
25	454.18	58.16	460.27	28.27	3.17	2.13
26	459.48	37.88	484.02	119.54	1.56	1.65
27	507.69	32.18	533.3	25.9	0.512	0.78
28	540.62	24.35	544.65	31.69	0.03	0.06
29	569.78	42.52	619.79	66.8	0.56	0.82
30	666.26	82.47	765.35	75.05	0.73	0.75
31	797.04	112.68	831.75	47.93	0.09	0.09
32	910.62	72.71	946.46	63.56	0.06	0.13
ε_∞				4.85		

*Calculated at the measured frequency: 7.1 GHz

Table 2. Calculated and measured dielectric properties of 1 mol % Sm_2O_3-doped $BaTi_4O_9$ ceramics

	Measured values	Calculated values
ε	37.54	38.52
$\mathrm{tg}\,\delta$	3.21E−4	1.70E−4

Compared with undoped $BaTi_4O_9$ ceramics, 1 mol % Sm-doped $BaTi_4O_9$ ceramics had a main binding energy peak nearer to the lower energy bar. Figure 6(a) could be fitted by 4 peaks, i.e., Ti2p3/2 at 457.65 eV, Ti2p1/2 at 463.21 of Ti^{4+} and Ti2p3/2 at 455.32, Ti2p1/2 at 461.22 of Ti^{3+}. But Fig. 6(b) of Sm_2O_3-doped $BaTi_4O_9$ could not be fitted by those four peaks, but by six peaks. The six peaks were 454.66, 457.11, 458.62, 461.14, 463.00, 464.43 eV. The peakes at 454.66 and 461.14 eV corresponded with the binding enery of Ti2p3/2, Ti2p1/2 of Ti^{2+}, respectively. The peaks at 457.11 and 463.00 eV were the binding energy of Ti2p3/2, Ti2p1/2 of Ti^{3+}, respectively. And the peaks at 458.62 and 464.43 eV were the binding energy of Ti2p3/2, Ti2p1/2 of Ti^{4+}, respectively.

The substitution of Ti^{4+} (0.68 nm) by Ti^{3+} (0.77 nm) and Ti^{2+} (0.90 nm) would bring about a great increase in unit cell volume, which could cancel out the increase by introduction of Sm^{3+} into Ba^{2+} sites. Also, XRD patterns had testified the fact. Such an abrupt increase of Ti^{3+} and Ti^{2+} content should be attributed to the doping of Sm_2O_3: after the doping of Sm_2O_3, equation of charge balance should be written as:

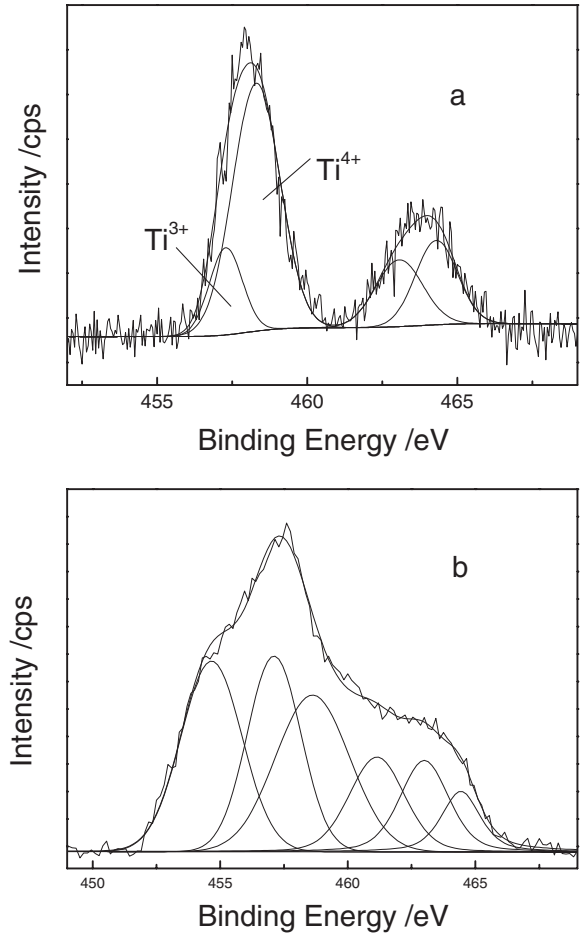

Fig. 6. XPS spectra of pure (a) and 1 mol % Sm-doped (b) $BaTi_4O_9$ ceramics.

$$[Ti'_{Ti}] + [Ti''_{Ti}] + [e'] = [Sm^{\bullet}_{Ba}] + [V^{\bullet\bullet}_{O}] + [h^{\bullet}]$$

Since the concentration of impurities was much higher than that of the eigen carriers and oxygen defects, the concentration of electron and holes could be ignored:

$$[Ti'_{Ti}] + [Ti''_{Ti}] \approx [Sm^{\bullet}_{Ba}]$$

The equation above could illustrate the abrupt increase of Ti^{3+} and Ti^{2+} content after the addition of Sm_2O_3. T. Negas had argued that the Ti^{3+} should be the cause of dielectric loss.[2] Therefore, the abrupt increase of dielectric loss should be attributed to the large content of Ti^{3+} and Ti^{2+}.

4. Conclusions

Sm_2O_3-doped $BaTi_4O_9$ ceramics was molded via a cool isostatic press process and sintered into disks at 1200°C for 6 hours. XRD and SEM were used to characterize the structural variation after Sm_2O_3 doping. The adding of Sm_2O_3 leaded to an increase of dielectric constant and dielectric loss, but a decrease of temperature coefficient. Curve fitting of FIRS was used to analyze the effect of anharmonic vibration modes on the dielectric loss, and the measured dielectric loss corresponded with the undoped samples. Results of XPS analysis showed that the increase of Ti^{3+} and Ti^{2+} in 1% Sm_2O_3-doped $BaTi_4O_9$ ceramics should be the cause of the increase of dielectric loss.

Acknowledgement The corresponding author gratefully acknowledges the financial support from the NUAA Research Funding (No. 2010159).

References

1) D. J. Masse, R. A. Pucel and D. W. Readey, *Proc. IEEE*, 59, 1628–1671 (1971).
2) T. Negas, *Am. Ceram. Soc. Bull.*, 72, 80–89 (1993).
3) G. Wolfram and H. E. Gobel, *Mater. Res. Bull.*, 16, 1455–1463 (1981).
4) M. Furuya and A. Ochi, *Jpn. J. Appl. Phys.*, 33, 5482–5487 (1994).
5) W. S. Kim, K. H. Yoon and E. S. Kim, *Mater. Res. Bull.*, 34, 2309–2317 (1999).
6) C. L. Huang, Y. B. Chen and S. H. Lin, *Solid-State Electron.*, 49, 1921–1924 (2005).
7) H. Zheng, D. Gyorgfalva and I. M. Reaney, *J. Mater. Sci.*, 40, 5207–5214 (2005).
8) Y. B. Chen, *J. Alloys Compd.*, 478, 657–660 (2009).
9) H. Ohsato, *J. Eur. Ceram. Soc.*, 21, 2703–2711 (2001).
10) S. G. Mhaisalkar, Readey and S. A. Akbar, *J. Am. Ceram. Soc.*, 74, 1894–1898 (1989).
11) S. G. Mhaisalkar, Readey and S. A. Akbar, *J. Solid State Chem.*, 95, 275–282 (1991).
12) Y. Cheng-Fu, T. Wen-Cheng, C. Ho-Hua, D. Chien-Chen and H. Chien-Jung, *J. Alloys Compd.*, 477, 673–676 (2009).
13) H. Xianli, W. Fuping, J. Zhaohua and S. Ying, *Jpn. J. Appl. Phys.*, 45, 868–871 (2006).
14) W. Fuping, L. Wenxu and S. Ying, *J. Sol-Gel Sci. Technol.*, 23, 39–43 (2002).
15) H. Ohsato, *J. Eur. Ceram. Soc.*, 21, 2703–2711 (2001).
16) J. A. Dean, "Lange's Chemistry Handbook Version 12th," Science Press of China, Beijing.
17) J. Pezelt, R. Zurmuhlen and A. Bell, *Ferroelectrics*, 133, 205–210 (1992).
18) J. Pezelt and S. Kmba, *Mater. Chem. Phys.*, 79, 175–180 (2003).